ELSEVIER

Polymer 42 (2001) 8703–8714

polymer

www.elsevier.com/locate/polymer

Temperature modulated DSC studies of melting and recrystallization in poly(ethylene-2,6-naphthalene dicarboxylate) (PEN) and blends with poly(ethylene terephthalate) (PET)

William G. Kampert*, Bryan B. Sauer

DuPont Central Research and Development Experimental Station, Wilmington, DE 19880-0356, USA

Received 16 January 2001; received in revised form 15 May 2001; accepted 17 May 2001

Abstract

The thermal properties of amorphous and melt crystallized poly(ethylene-2,6-naphthalene dicarboxylate) (PEN) and its blends with poly(ethylene terephthalate) (PET) were investigated. Temperature modulated DSC (TMDSC) was used over a broad range of annealing times and temperatures. PEN under all moderate temperature crystallization conditions was found to exhibit secondary crystal melting in the low endotherm region, followed by melting of primary crystals superimposed with a large endotherm due to melting of DSC scan-induced recrystallized species. The exothermic signal due to recrystallization was separated into the TMDSC non-reversing signal. Annealing time had a small effect on thermal properties at moderate annealing temperatures, and varying the annealing temperature had a larger effect on the recrystallization properties above the annealing temperature. The results show that TMDSC provides excellent resolution of recrystallization and related events compared to standard DSC. Blends of PEN and PET were evaluated as a function of melt blending time, and the phase properties were studied at 260 and 285°C and related to transesterification reactions. The evolution from a phase separated mixture to a single phase but still crystallizable copolymer, to finally a non-crystallizable copolymer with a higher degree of randomness was studied. The crystallization properties measured using TMDSC were contrasted with those of PEN.

Keywords: Poly(ethylene-2,6-naphthalene dicarboxylate); Poly(ethylene terephthalate); Blends

1. Introduction

Substantial efforts in recent years have been devoted to the study of thermal properties of relevant industrial semi-crystalline polymers such as poly(ethylene terephthalate) (PET), poly(ethylene-2,6-naphthalene dicarboxylate) (PEN), and poly(oxy-1,4-phenyleneoxy-1,4-phenylenecarbonyl-1,4-phenylene) (PEEK). These high temperature polymers are used in a variety of engineering applications; the fundamental understanding of their melting and recrystallization behavior correlated with performance in a variety of applications. PEN contains a naphthalene ring in its backbone making it more rigid than PET. Many researchers have studied the thermal properties [1–5]. It has a glass transition of 117°C with an equilibrium melting point of 337°C [1]. Buchner et al. [2] extensively studied the development of the two different crystal forms (α and β) of PEN. Cheng and Wunderlich [1] systematically characterized the heat capacity of PEN over a wide temperature range to describe its melting behavior and used glass transition strengths and percent crystallinities to characterize morphological development. There is some controversy in the determination of the heat of fusion of 100% crystalline PEN (ΔH_f) with values of 103 [1], 190 [2], and 170 J g^{-1} [6]. The value of ΔH_f is very important for calculating percent crystallinities and various rigid fractions [1,6].

Temperature modulated DSC (TMDSC) is a relatively new technique [7–10] that superimposes a low frequency small amplitude temperature oscillation onto a linear heating ramp of standard DSC. One can obtain the 'total' heat flow like that in conventional DSC. By deconvolution the total heat flow can be separated into a heat capacity-related (reversing) component and a time-dependent non-reversing (NR) component [7–10]. The reversing signal provides excellent resolution of the glass transition (Table 1) by separating the heat capacity from other non-reversing processes such as enthalpy relaxation and crystallization as is well known in the literature [4,6,7–10]. However, endothermic melting can also be detected in the reversing signal as long as the endothermic heat flow remains in phase with the imposed oscillation [11]. All exothermic behavior is detected only in the NR signal because the 'slow' kinetics

* Corresponding author.

0032-3861/01/$ - see front matter
PII: S0032-3861(01)00364-0

Table 1
DSC and TMDSC data from amorphous and isothermally melt crystallized PEN samples at various heating rates including glass transition temperatures, and heats of melting and crystallization. All temperatures in °C, ΔH in J g^{-1}, and ΔC_p in J g^{-1} K^{-1}

	ΔC_p	T_g	$\Delta H_{endo,low}$	$\Delta H_{exo,NR}$	$\Delta H_{endo,NR}$	$\Delta H_{endo,R}$	ΔH_{total}	$\%X$[a]
Amorphous, 2°C/min	0.255	123.6	–	84.7	3.9	80.8	0	0
170°C, 6 min, 2°C/min	0.144	126	–	46	18	58	30	17.6
170°C, 80 min, 2°C/min	0.018	129	1	37.9	17	60.3	40.5	23.8
170°C, 18 h, 2°C/min	0.0044	129.5	1.6	27.9	18.1	57.1	49	28.8
170°C, 5 days, 2°C/min	0.06	132	2.1	18	15.9	61.2	61.2	36
210°C, 2 h, 2°C/min	0.131	121.5	1.0	21	15.1	54.6	48.7	28.6
210°C, 2 h, 10°C/min[b]	0.081	125.7	–	–	54.4	–	54.4	32
210°C, 2 h, 40°C/min[b]	0.092	127.7	6.7	–	50.2	–	50.2	29.5
210°C, 17 h, 2°C/min	0.06	130	6.9	6.7	14.7	54.6	69.5	40.9
210°C, 17 h, 10°C/min[b]	0.054	129	–	–	68.5	–	68.5	40.3
210°C, 17 h, 40°C/min[b]	0.0675	140	–	–	64.9	–	64.9	38.2
240°C, 30 min, 2°C/min	0.099	124	–	3.7	30.5	27.8	54.6	32.1
240°C, 18 h, 2°C/min	0.073	128.5	–	–	54.4	15.7	70.1	41.2
265°C, 24 h, 2°C/min	0.075	124	–	–	52.7	11.7	64.4	37.9
265°C, 5days, 2°C/min	0.06	125	–	–	62.8	6.55	69.35	40.8

[a] Percent crystallinities were calculated from heat of fusion for 100% crystalline PEN of 170 J g^{-1} [6].
[b] For the 10 and 40°C/min heating rate scans, table entries refer to values from the total DSC heat flow curve.

cause a heat flow response which is not in phase with the temperature oscillation [7–11]. This helps in the separation of thermal events. Unfortunately, the non-reversing signal can contain components of both exothermic and endothermic processes which makes resolution of some thermal events difficult [6,11,12].

There have been many efforts devoted to understanding the complexity of the melting and recrystallization behavior of PEN [1–6] and other related polymers where recrystallization refers to the metastability of crystals as the DSC heating scan modifies the starting morphology leading to higher melting crystals [13]. There seems to be a lack of agreement in the literature for a specific model for multiple endotherms in DSC. We feel an accurate description of the multiple endotherms in PET was given by Zhou et al. [14]. Using standard DSC, they qualitatively incorporated both dual crystal populations and melting and recrystallization into their analysis. Their data [14] were best described by early melting of secondary crystals which contribute to the low endotherm region, melting of primary crystals to the middle endotherm which is always 'present' but not always distinguishable in the total DSC curve, and the final endotherm which contains significant contributions from the recrystallized species formed during heating at normal heating rates. With the increased sensitivity of TMDSC and an independent rapid heating rate technique for determining melting points without recrystallization contributions [4,6,12], we have also recently shown that, independent of the number of distinct endotherms detected in the total DSC data in PET, PEN, and PEEK, three melting processes are needed to characterize the typical thermal scan of these polymers. Exceptions exist including high temperature annealed PET [15] and PEN [2,4]. Other authors have used DSC and temperature scanning X-ray as complementary techniques to detect melting and recrystallization events [15–17].

One of the first studies of PEN was that of Cheng and Wunderlich [1] using standard DSC to describe the thermal analysis of various glass and melt crystallized samples. They found triple melting behavior in some samples and investigated the effect of crystallization temperature on morphological development. They also observed decreased recrystallization (DSC heating induced reorganization) with increased heating rate for samples annealed below 227°C. Buchner et al. [2] investigated the formation of the two different crystal modifications of PEN (α and β) under various crystallization conditions. Only the α form develops under crystallization temperatures up to 200°C, and above this temperature the β form is detected. They also attributed the lowest temperature endotherm as being due to partial melting followed by recrystallization, and described evidence for recrystallization contributions to the final melting endotherm. Medellin-Rodriguez et al. [3] observed triple melting behavior in various isothermal crystallized PEN, PET, and PEEK samples. Their description of the sequence of thermal events included secondarily crystallized material melting in the first two endotherms and primary crystals melting in the highest temperature endotherm. They utilized standard DSC at 10°C/min, X-ray, and optical microscopy. Denchev et al. [5] studied isothermally crystallized PEN from the glass at different times and temperatures. Slow heating (2°C/min) from the amorphous glass to the isothermal annealing temperature allows one to develop an unstable morphology (due to formation of a broad range of crystals with different melting points as one slowly heats through the crystallization region to the desired annealing temperature). The unstable morphology then evolves considerably with time. Rapid heating (200°C/min) from the amorphous glass to the isothermal annealing temperature provides a more 'stable' morphology similar to melt crystallization, but we will show

here that almost all isothermal annealing temperatures except the highest ones lead to some metastability of the morphology which strongly contributes to the final DSC melting region. The recrystallization and melting processes in PEN were examined along with the morphological features by small angle X-ray scattering. Dual lamellar populations were observed depending on the temperature and time of crystallization [5]. Here we apply TMDSC in an effort to provide improved resolution of the recrystallization and melting in isothermally melt annealed PEN. The improved resolution of glass transitions by TMDSC and DSC will also be utilized in studies of phase behavior of PET/PEN blends as well as the crystallization and recrystallization behavior as a function of the extent of transesterification of the two components.

2. Experimental

2.1. Materials

PEN with a weight average molecular weight (M_w) of about 45,000 was obtained from Teijin Chemical. PET was obtained from DuPont with a weight average molecular weight of about 50,000. The pellets were melted to make new films ~0.5 mm thick. For melt crystallization, after heating the films to 290°C for 2 min on a hot plate, the sample was quenched into the small brass chamber at the annealing temperature for the desired time. After annealing they were quenched to room temperature at ~500°C/min.

2.2. Methods

A TA Instruments (New Castle, DE) 2920 DSC was used in these experiments. Most experiments utilized TMDSC heating ramps of 2°C/min with a modulation amplitude of 0.32°C with a period of 60 s based upon the recommended specifications in an effort to obtain 'heating only' modulated temperature profiles [18,19]. The modulation temperature amplitude is small relative to the underlying heating rate, so there is no local cooling during the standard TMDSC scan which is referred to as heating-only. Data analysis software was supplied by the manufacturer [18]. Standard DSC was also performed at higher heating rates of 10 and 40°C/min. A N_2 purge was used for all experiments. Careful baseline calibration is critical for these films exhibiting broad and weak transitions and was performed regularly at the different heating rates [12]. To reduce heat flow lags, typical sample masses of 3–5 mg consisting of flat single layer polymer films were used.

Amplitudes were always set to levels where the profile is heating-only [12,18] as described in the operating procedures for the modulated DSC (T.A. Instruments 2920). For example, the amplitudes were set to 0.32°C for a 60 s period and 0.16°C for a 30 s period when using a heating rate of 2°C/min. A strong frequency (= 1/modulation period) dependence of the reversing endothermic melting signal has been demonstrated recently [19–21]. Since the total TMDSC signal is quantitative and independent of frequency, the NR signal in the melting region is also frequency dependent (recall that, Total = R + NR). Differences in total, R, and NR data due to variations of underlying heating rate are also important. In other words, the extent of recrystallization can be affected by scan rate and this is a parameter, which actually influences the physical state of the sample and is addressed later. To analyze data taken as operating parameters such as modulation period are varied, Toda et al. [19] have used a model which considers time constants for melting which vary with temperature through the melting region in PET and other materials.

Temperature gradients within the sample and other effects described previously [22] can contribute to nonlinearity of the heat flow. The following discussion shows how we have attempted to verify that temperature gradients were minimal [21]. Also, evaluation of data taken using different modulation amplitudes and examination of time dependent modulated heat flow data verified that precise data can be obtained over a certain range of modulation periods, amplitudes, sample thicknesses, and underlying heating rates. For example, a low modulation temperature amplitude of 0.265°C, heating rate of 1°C/min, and a small sample size of 3.1 mg (Fig. 3) was used to attain even more ideal conditions [21,23] than the typical 2°C/min 'standard' conditions used for the majority of the experiments presented here. Fig. 3 gives the raw modulated heat flow data for a 210°C, 1 h melt crystallized PET sample and the features of the processed curves including total, R, and NR signals are also included in the plot. Integration of the R and NR signals in Fig. 3 gives the same quantities within experimental error as those obtained from another sample with the same thermal history studied using our standard 2°C/min heating rate with a slightly higher amplitude. Changing the modulation period causes a substantial variation in the magnitude of the reversing data in the melting region [19–21], and our data do not cover a broad enough range to see such differences. To interpret other important features of Fig. 3, note that the heat flow amplitude is related to the reversing signal, and the NR curve is approximately equal to the zero heating rate portion of each cycle which correspond to the uppermost peaks of each modulation period [18]. One can see a slight temperature offset between the calculated NR curve and the zero heating rate portions of the modulated heat flow data due to the transform used by the software.

The amorphous PEN sample in Fig. 1 and the 170°C annealed PEN sample in Fig. 2 (at various annealing times) display a high temperature endotherm in the NR signal around 270°C. The integrated reversing (melting endotherm) and nonreversing (exothermic crystallization and melting endotherm) signals in Fig. 2 gave essentially constant values within an experimental error of about 10% as long as temperature gradients were minimized. For example, we covered a range which included slight

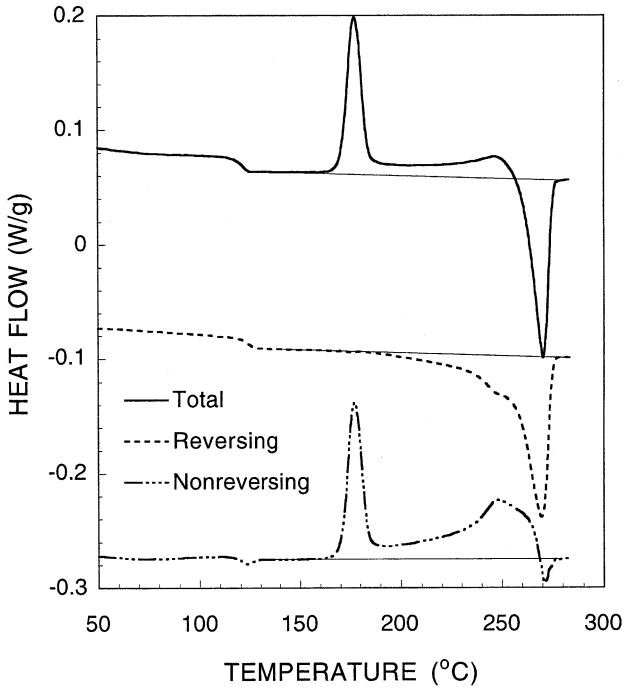

Fig. 1. Total (solid), reversing (dash) and non-reversing (dot-dash) curves of TMDSC data with a 2°C/min heating rate for initially amorphous PEN. The total signal is the sum of the R and NR signals. The curves have been shifted vertically for clarity. The exothermic direction is upward in the plot.

variations in frequency and relatively large changes in sample mass and thickness. For a 210°C (1 h) melt crystallized PET sample the following experimental conditions led to integrated quantities which were constant to within about 10% experimental variability: Run #1 (2.6 mg, 90 μm thickness, 30 s period, 3.5°C/min heating rate), Run #2 (1.6 mg, 70 μm, 60 s, 2°C/min), Run #3 (6 mg, 220 μm, 60 s, 2°C/min), and Run #4 (3.1 mg, 140 μm, 100 s, 1°C/min, data for Run #4 given in Fig. 3). Toda et al. [19] provide a much more systematic study of frequency and underlying heating rate effects on the melting region of initially amorphous PET. Close examination of their work (Fig. 5) [19] shows why our particular choices of frequency and underlying heating rates in these four examples lead to qualitatively similar results, but the data we present in the figures and Table 1 are specific only to the chosen TMDSC operating parameters and thus are only qualitative.

Returning to the issue of thermal gradients, Run #5 (5.6 mg, 210 μm, 60 s, 3.5°C/min) gave slightly inaccurate results because of an insufficient number of modulation cycles through the narrow endotherms, especially the highest temperature nonreversing endotherms such as those at 270°C in Figs. 1 and 2 and 258°C in Fig. 3. Run #6 (10 mg, 400 μm, 30 s, 3.5°C/min) and Run #7 (10 mg, 400 μm, 60 s, 3.5°C/min) were adversely affected by thermal gradients due to large sample thicknesses and relatively high modulation frequencies. Although the reversing and especially the nonreversing signals were inaccurate, the total was relatively accurate.

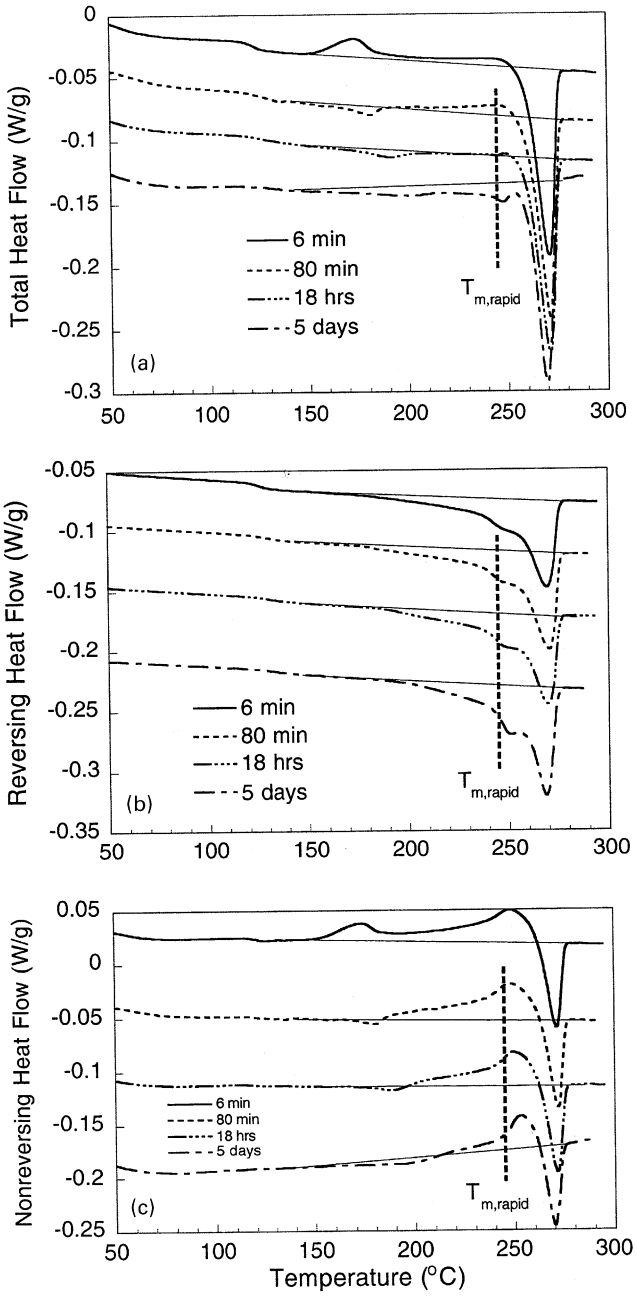

Fig. 2. (a) Total curves of TMDSC data for PEN heated at 2°C/min after being melt crystallized at 170°C for 6 min (solid line), 80 min (dashed line), 18 h (dot-dot-dot-dash line), and 5 days (dot-dashed line). The curves have been shifted vertically for clarity. The total signal is the sum of the R and NR signals. The melting temperature of crystals 'originally' present equals about 245°C for the 80 min sample and was independently measured by the rapid heating rate technique, and this temperature is indicated by the dashed vertical line (see text). The exothermic direction is upward in the plots. (b) Corresponding reversing heat flow. (c) Corresponding nonreversing heat flow.

2.3. Blending procedure

The melt blending procedure for small quantities only has been described previously [24]. The blending method consists of pressing and shearing molten polymer films

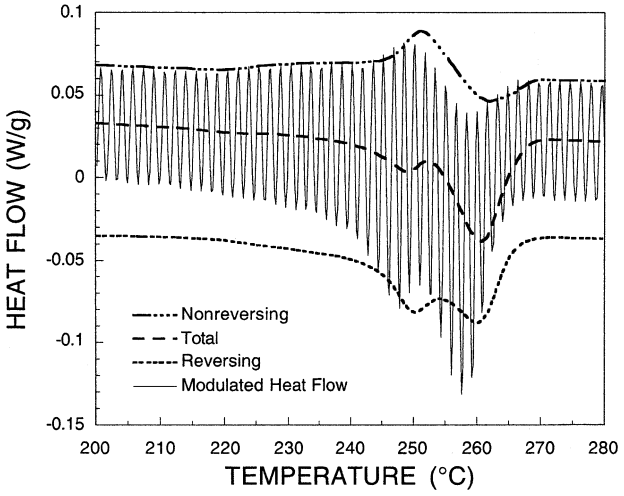

Fig. 3. Non-reversing (dot-dot-dot-dash), total (large dash), reversing (small dash) and raw modulated heat flow (solid) curves of TMDSC data at a 1°C/min heating rate for PET melt crystallized at 210°C for 1 h. The modulation amplitude was 0.265°C with a period of 100 s. The sample size was 3.1 mg. The total signal is the sum of the R and NR signals. The exothermic direction is upward in the plot.

(~0.05 g total) on a hot plate between sheets of Kapton® polyimide and then quenching. The solidified sample releases easily from the Kapton®, is folded, and the process repeated 5–10 times. The total exposure to the high temperatures in the melt for four blending cycles is typically only 5 s. Due to the small film areas ($A \sim 200\ mm^2$), relatively high shear and elongational forces can be applied by hand. Equilibration of the blend phase morphology can be tested by obtaining a DSC trace on a blend, and then reblending the same sample a few more times before performing DSC a final time. In this way one can check for further changes in T_g (i.e. changes in phase compositions) as well as thermal degradation [24].

3. Results

3.1. TMDSC of amorphous samples

The thermal response and morphology developed during heating of initially amorphous PEN provides a useful system for understanding the detailed morphological changes that occur with increasing temperature. Amorphous PEN is heated at 2°C/min in TMDSC scans that have a heating-only amplitude of 0.32°C with a modulation frequency of 60 s (Fig. 1). The total heat flow signal is equivalent to a standard DSC, even though it was obtained by a slightly different averaging procedure using the TMDSC technique. The total heat flow curve shows the glass transition, immediately followed by the nominal cold crystallization peak. This is followed by the well-known continuous melting and recrystallization of these just formed crystals [6,25–27]. Continuous recrystallization due to the heating scan is detected starting at ~177°C by the small increase of the total signal over the baseline. This exothermic activity is more dramatically illustrated in the nonreversing signal as the curve stays above the baseline over a broad temperature range above ~177°C until final melting at 271°C. The peak melting temperature for the total heat flow curve is 270°C. The glass transition is separated into the reversing signal at 124°C. Addition of the reversing and non-reversing signal gives the total signal, and this integrated total signal gives a heat of fusion (ΔH) equal to approximately zero, as should be the case for an initially amorphous sample (Table 1).

The nonreversing curve characterizes the cold crystallization exotherm at about 177°C, which appears well after T_g. In addition, the ongoing process of recrystallization (appearing as exothermic behavior in the NR curve) follows the cold crystallization peak and does not end until the very end of the melting. This 2°C/min scan exhibits a small endothermic melting event in the nonreversing signal at around 271°C (Fig. 1). At this lower heating rate, the crystals have more time during the heating scan to perfect; and the properties of these crystals, which separate the melting into the NR signal will be discussed below. The non-reversing curve can contain both endothermic and exothermic behavior [4].

3.2. TMDSC study of low temperature isothermally annealed PEN

With selection of crystallization conditions (both temperature and time), the combination of standard DSC with TMDSC can provide characterization of the morphology developed as well as melting and recrystallization behavior. PEN was melt crystallized at different times at 170°C and the TMDSC scans at 2°C/min in Fig. 2 show similar trends for all four annealing times. To understand DSC or TMDSC in general, one should consider the sequence of events starting with secondary crystal melting in the low endotherm, continuous recrystallization of secondary and low melting primary fractions, followed by melting of the primary crystals, combined with melting of the recrystallized species contributing to the endotherm at the highest temperatures [14]. Specifically for TMDSC, the low endotherm consists of a non-reversing melting endotherm which starts a few degrees before the endothermic drop in the reversing signal at about 180°C (Fig. 2). This is immediately followed by relatively high levels of exothermic recrystallization for all four samples, which mostly obscure the broad melting endotherm of the primary crystals in the total heat flow signal for these samples in Fig. 2 at about 245°C. Some indication of the melting of primary crystals is detected in the reversing endotherm region around 245°C. This complicated behavior helps to resolve the controversy in the literature regarding interpretation of standard DSC in the melting region. The TMDSC curves and quantities in Table 1 must be taken as qualitative because the R and NR signals will change with a variation of the TMDSC

operating parameters in the melting region as was discussed in Section 2. The general features described here along with differences between samples with different thermal history do provide valuable relative comparisons because all were measured under the same TMDSC conditions.

After 6 min at 170°C, the curve in Fig. 2 still displays a sharp cold crystallization peak in the total heat flow after Tg followed by broad recrystallization of these just formed crystals as well as the primary crystals (seen as the total heat flow curve remaining above the baseline) followed by the final melting endotherm. The total heat of fusion (ΔH) for this sample is 30 J g^{-1} (Table 1). This selection of annealing temperature with its large degree of undercooling provides a kinetically restricted growth environment. There is not a separable low endotherm in the total or nonreversing signals for the 6 min annealed sample; but, we do observe the cold crystallization peak in the nonreversing signal. This is not seen in the sample annealed for 80 min due to more complete spherulitic space filling. Consequently, a low endotherm of 1 J g^{-1} is resolvable in the total and nonreversing signals and ΔH for the 80 min annealed sample increases to 40.5 J g^{-1}. After this low endotherm in the NR signal, the just melted secondary and low melting primary crystals recrystallize and contribute to the exothermic signal in the NR curve. This process is followed by final melting of these perfected species in the NR endotherm at 271°C. These trends continue as the annealing time is further increased to 18 h and 5 days. The low endotherm rises to 1.6 and 2.1 J g^{-1}, respectively, as well as ΔH changing to 49 and 61 J g^{-1} (Table 1). With increasing annealing time, the net nonreversing exothermic behavior in the samples is decreased owing to the better perfection of the crystal morphology with subsequently lower DSC-heating induced reperfection. Integrated values for the NR_{exo} drop from 46 J g^{-1} at 8 min to 18 J g^{-1} at 5 days. This impacts the total heat flow as the curve starts to fall below the baseline for the 18 h sample above 200°C. Regardless, the data and especially the NR curves dramatically illustrate the strong recrystallization behavior which is not at all obvious from the total signals. The reversing endotherms remain fairly constant over this time series with little shift in the integrated ΔHs (~60 J g^{-1}) or final melting points (270°C) as seen in Table 1. However, the melting of the primary crystals formed at this annealing temperature appears as a shoulder in the reversing curve around 245°C and is only a separable 'peak' in the total curve in the 5-day sample.

3.3. Variable heating rate DSC

Samples were isothermally melt crystallized and quenched below T_g as described in Section 2.2. Although total heat flow in TMDSC scans is equivalent to that obtained in a standard DSC, TMDSC is limited to low heating rates (~5°C/min or lower) in order to have adequate sensitivity and resolution. Therefore, a variable heating rate study using standard DSC was executed for a 210°C (2 h) melt annealed PEN sample. In Fig. 4, the standard DSC scans display the response to heating rates of 2, 10, and 40°C/min. The glass transition is clearly evident and increases in temperature with heating rate from 121.5°C at 2°C/min to 126°C at 10°C/min to 128°C at 40°C/min (Table 1). Following the glass transition, triple melting behavior is approximately seen for all three heating rates. The low endotherms (due to the melting of secondary crystals) in the total curves rise in temperature with increasing heating rate [12,28], and the highest endotherm decreases dramatically in peak melting temperature with increasing heating rate as shown earlier in many studies [4,29,30]. The middle endotherm is the melting of initially formed primary crystals, which overlaps with the highest endotherm resulting from the large fraction of higher melting crystals formed by reorganization during DSC heating, as was also studied in some detail in the reversing data of Fig. 2. Higher heating rates suppress the recrystallization contribution and shift the final melting point down (Fig. 4) as is well known [29,30], and help to confirm the interpretation of TMDSC that we have proposed.

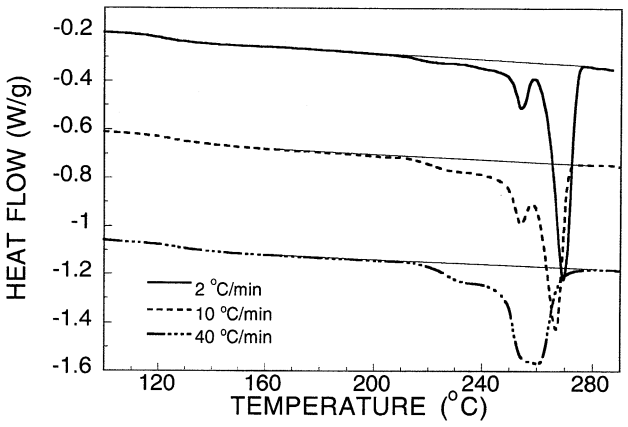

Fig. 4. Standard DSC curves for PEN heated at 2°C/min (solid line), 10°C/min (dashed line), and 40°C/min (dot-dash line) after being crystallized for 2 h at 210°C. The vertical axes have been normalized by a factor proportional to heating rate. The curves have been slightly shifted vertically for clarity. The higher endotherm decreases in peak temperature with increased heating rate. The exothermic direction is upward in the plot.

The low endotherm or melting of secondary crystals appears as a shoulder at 225°C in the 2°C/min heating rate scan (Fig. 4). This has been shown previously [4] to be modified by the nonreversing recrystallization exotherm occurring immediately following this endotherm (Fig. 5); and again, the low heating rate enhances this recrystallization contribution so the low endotherm can effectively change in magnitude at the different heating rates. This low endotherm appears again as a shoulder in the 10°C/min data at a temperature of 227.5°C and in the 40°C/min scan at 231°C. Alternatively, the highest endotherm decreases in peak temperature with increasing heating rate changing from 270°C (2°C/min) to 267°C (10°C/min)

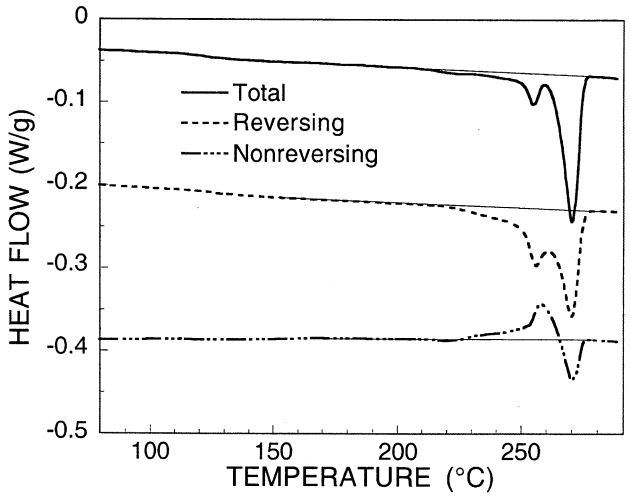

Fig. 5. Total (solid), reversing (dash) and non-reversing (dot-dash) curves of TMDSC data at a 2°C/min heating rate for PEN crystallized at 210°C for 2 h. The total signal is the sum of the R and NR signals and is equivalent to a standard DSC curve. The curves have been slightly shifted vertically for clarity. The exothermic direction is upward in the plot.

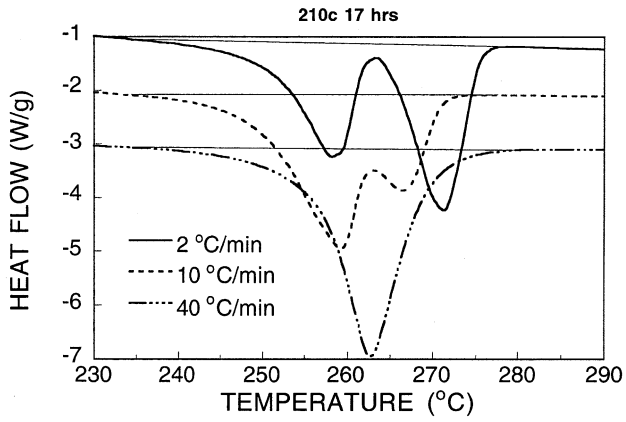

Fig. 6. Standard DSC curves for PEN heated at 2°C/min (solid line), 10°C/min (dashed line), and 40°C/min (dot-dash line) after being crystallized for 17 h at 210°C. The vertical axes have been normalized by a factor proportional to heating rate. The curves have been slightly shifted vertically for clarity. The higher endotherm decreases in peak temperature and size with increased heating rate and merges with the lower temperature endotherm into a single peak in the 40°C/min scan.

to 260°C (40°C/min). The melting of primary crystals characterized in the middle endotherm occurs at 254°C in the 2 and 10°C/min heating scans; but, in the 40°C/min heating rate curve, the middle and highest endotherms merge into a single melting peak with the melting of recrystallized species becoming much weaker because there was less time for recrystallization. This overlap of thermal events at high heating rates is well known [13]. The percent crystallinities for the different heating rates show good agreement where all values fall in the 29–32% range (Table 1).

Fig. 5 is the TMDSC data for the sample studied in Fig. 4 at 2°C/min with triple endothermic behavior in the total signal. The lowest endotherm is the melting of secondary crystals (appearing as a shoulder in the total signal) was discussed previously. The middle endotherm is the melting of primary crystals and the highest endotherm is the melting of recrystallized species. One can detect the low endotherm in the nonreversing curve of Fig. 5 at 220°C immediately followed by recrystallization of these just melted species. The peak temperature of this exotherm is at 257.5°C. The nonreversing curve then displays the endothermic melting of a fraction of recrystallized species with a small minimum at 270°C. The reversing curve in Fig. 5 shows the onset of primary crystal melting with a peak temperature of 256°C followed by melting of recrystallized species with a peak temperature of 270°C. Since the total heat flow is the sum of the reversing and nonreversing curves, the resulting total curve displays no exothermic behavior.

The annealing time was increased to 17 h at 210°C for the next variable heating rate study. With this increased time, the percent crystallinities rise to 39 ± 2%. In the heating rate data shown in Fig. 6, the 2 and 10°C/min scans display a double melting endotherm whereas the 40°C/min scan exhibits only one endotherm as the recrystallization is suppressed. The lower temperature endotherm is mainly due to the melting of primary crystals formed during the annealing at 210°C (Fig. 6).

Fig. 7 contains the TMDSC data of the sample studied in Fig. 6 at 2°C/min and shows the low temperature endotherm region with superimposed melting of secondary and primary crystals. One can observe that the middle endotherm in the reversing signal, which is the melting of primary crystals, is much larger than the middle endotherms of Fig. 4 because of the increased annealing time. Also, the middle endotherm in the total heat flow is dominated by a reversing endothermic contribution. These annealing conditions develop a crystal morphology where the stability of the primary crystals contributes to melting which is fully resolvable in the reversing signal because it is in phase with the modulation.

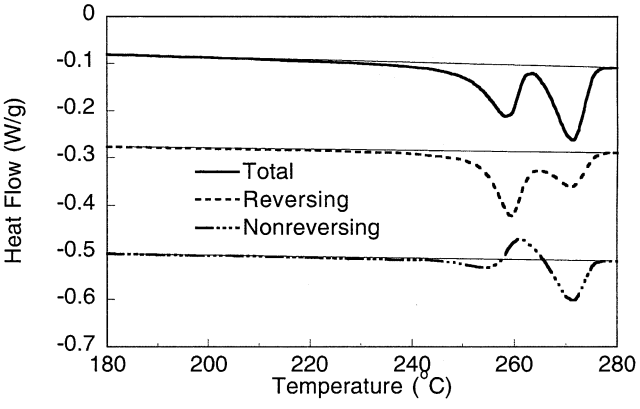

Fig. 7. Total (solid), reversing (dash) and non-reversing (dot-dash) curves of TMDSC data at a 2°C/min heating rate for PEN crystallized at 210°C for 17 h. The total signal is the sum of the R and NR signals and is equivalent to a standard DSC curve. The curves have been slightly shifted vertically for clarity.

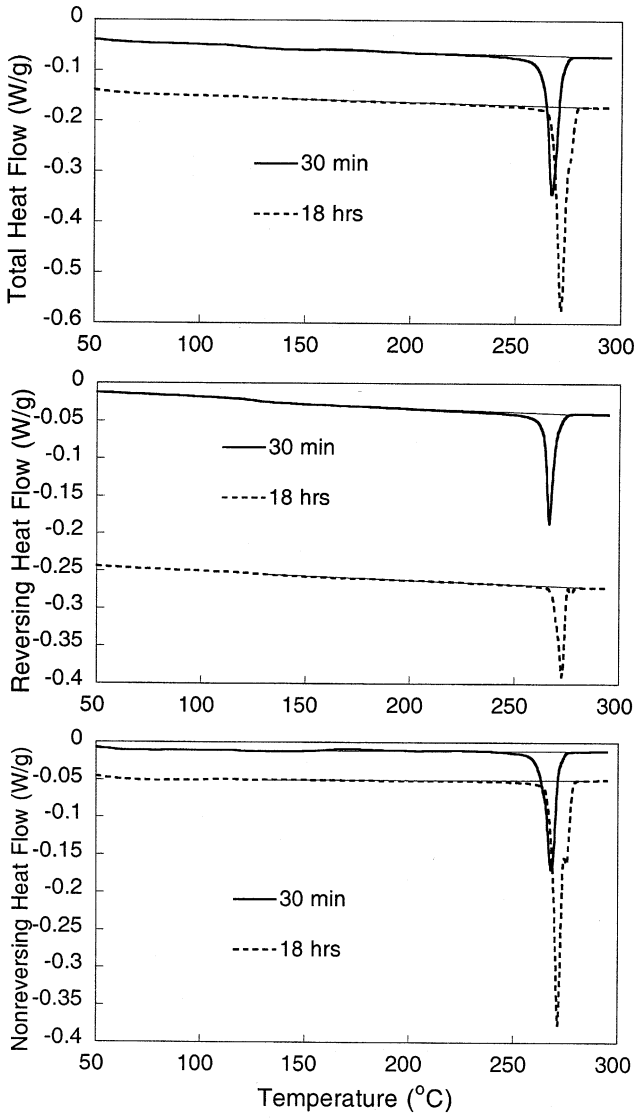

Fig. 8. (A) Total heat flow curves of TMDSC data at 2°C/min for PEN crystallized at 240°C for 30 min (solid) and 18 h (dash). The curves have been shifted vertically for clarity. The peak melting temperature increases from 267.2 to 271.8°C with annealing time. (B) Corresponding reversing heat flow. (C) Corresponding nonreversing heat flow.

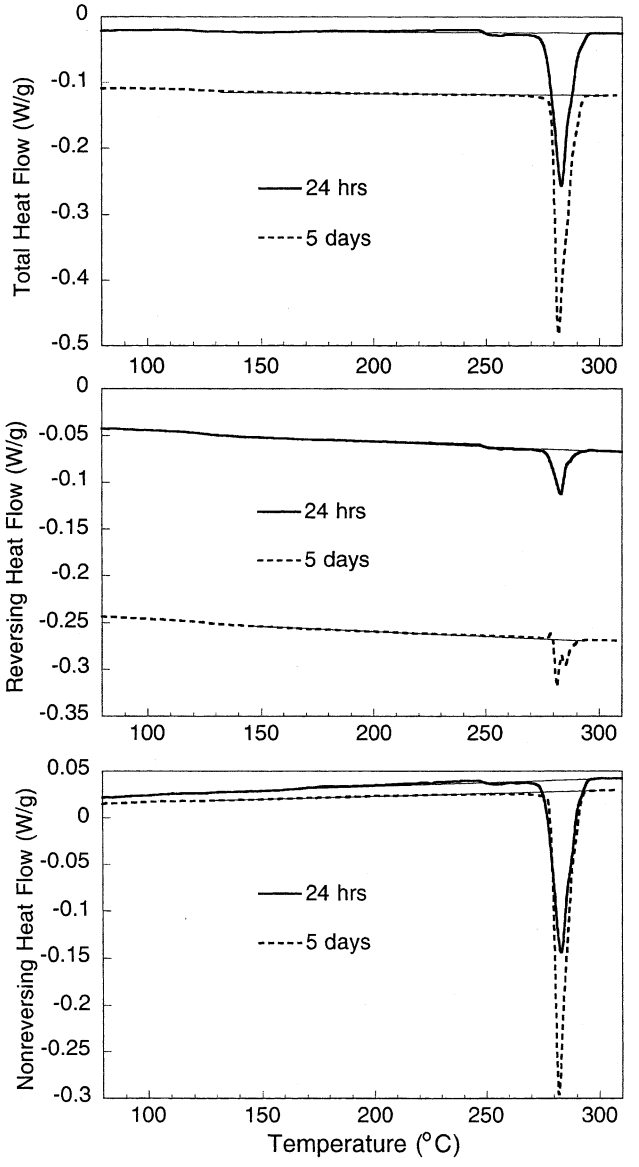

Fig. 9. (A) Total heat flow curves of TMDSC data for PEN crystallized at 265°C for 24 h (solid) and 5 days (dash). The overall heating rate is 2°C/min. The curves have been shifted vertically for clarity. The peak melting temperature does not shift with annealing time over this range. (B) Corresponding reversing heat flow. (C) Corresponding nonreversing heat flow.

Secondary crystal melting is well separated into the NR signal (Fig. 7) because of the superheating of these species [12,28], and this explains the distinct endothermic peak at 254°C in the NR curve even though the total curve contains no evidence of this endotherm. Immediately following this endotherm in the NR is the exotherm of the primary and secondary recrystallization; and after this, the final melting endotherms of the recrystallized species detected in both the reversing and NR curves with peak melting temperatures of 271°C.

3.4. TMDSC studies of higher temperature isothermally annealed PEN

In comparison to the previous section on isothermally annealed samples annealed with a large degree amount of undercooling, much higher temperatures of 240°C were used. PEN was held for 30 min and 18 h and the TMDSC data at 2°C/min are shown in Fig. 8. From the total heat flow curve, the peak melting temperature rises with annealing time from 267 to 272°C. The total heat of fusion also increases as ΔH changes from 55 to 70 J g^{-1} as indicated in Table 1. In the 30 min sample, both the reversing and nonreversing signals contribute about 50% of the total heat of fusion whereas, in the 18 h sample, about 78% of the total comes from the nonreversing signal. The increased time at this elevated annealing temperature allows perfection of the primary and secondary crystals

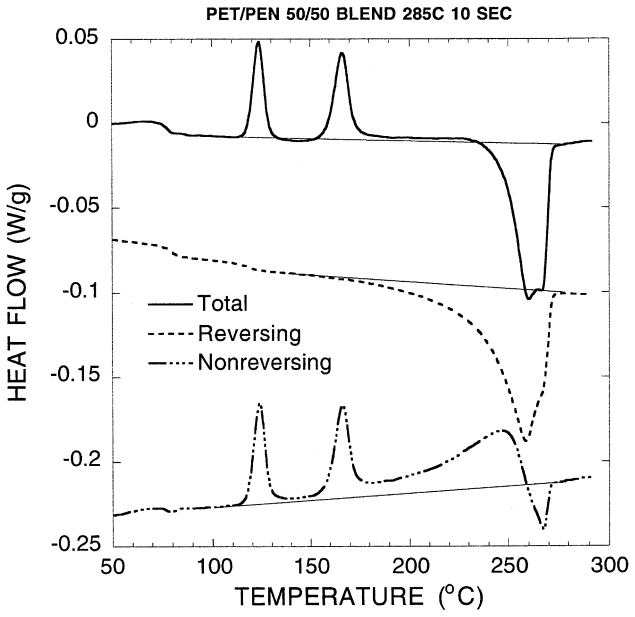

Fig. 10. Total (solid), reversing (dash) and non-reversing (dot-dash) curves of TMDSC data at a 2°C/min heating rate for a PET/PEN (50/50) blend mixed at 285°C for 10 s. The total signal is the sum of the R and NR signals and is equivalent to a standard DSC curve. The curves have been slightly shifted vertically for clarity. Both glass transitions of the pure species are observable in the reversing signal as well as the nonreversing signal having separate crystallization exotherms of the pure species.

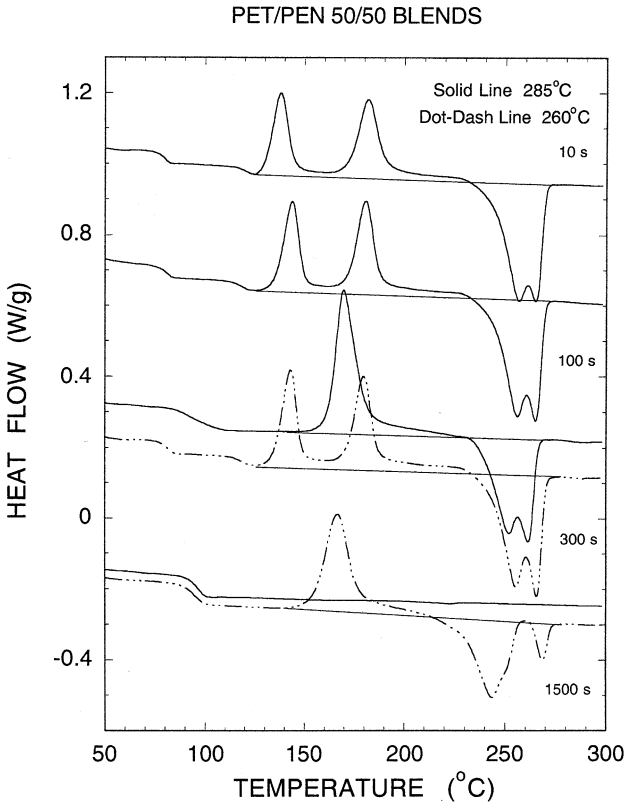

Fig. 11. Standard DSC curves at 10°C/min for PET/PEN (50/50) blends after being mixed for various times at 285°C (solid) and 260°C (dot-dash). The shortest mixing times are at the top and increase in mixing time with the longest ones at the bottom. The curves have been slightly shifted vertically for clarity. The blends are incompatible until about 5 min at 285°C and 25 min at 260°C.

as seen by the increased crystallinity and elevated melting points [2,4].

An even higher annealing temperature of 265°C was used to further investigate the development of crystal morphology. Two samples were held for 1 and 5 days at this temperature and gave ΔH values of 64 and 69 J g^{-1}, respectively (Table 1). The data at 2°C/min shown in Fig. 9 indicate the melting points are almost identical for the two samples (little increase in perfection at the longer time) and most of the melting is nonreversing. The melting points of the samples are increased to 282–283°C.

4. Blends

For the blends, TMDSC studies of each sample were not necessary because of strong similarities in the general features of the TMDSC results. A typical experiment on a phase-separated blend allows one to emphasize the two most important features of TMDSC. These include separation of the glass transitions into the reversing signal. Fig. 10 shows that the upper glass transition is not detectable in the total signal because of the overlap with the cold crystallization exotherms. The other feature is the characterization of the strong recrystallization of both components, which is seen in the NR signal between about 180 and 260°C. The melting of both components is partially distinguished in the total and reversing signals, with the PEN fraction melting at slightly higher temperatures on average (Fig. 10). As with isothermally annealed homopolymers, the strong recrystallization seen directly in the NR signal between 180 and 260°C strongly modifies the final melting region.

Fig. 11 gives total DSC curves (10°C/min) for several 50/50 blends formed at two blending temperatures. At relatively high blending temperatures of 285°C, even though mixing provides a uniform domain dispersion with phase separated domains on the order of less than 1 μm, the system is highly incompatible at early times and the components have phase purities and thermal properties almost identical to the pure components. This novel blending method was verified to provide excellent and complete dispersion and mixing in hundreds of other experiments on miscible and partially miscible high temperature polymers [24,31], and single phase blends could be formed in about 5 s of total 'mixing' time in cases where the components were thermodynamically miscible. We believe it provides unambiguous evidence that PET and PEN are incompatible in the homopolymer form. The 260°C (300 s) is even better verification where the uniform domain size of less than 1 μm is reached in the first 5 s of mixing, and even after 295 more seconds of continuous mixing almost no decrease in phase purity is observed, i.e. after

Table 2
DSC data for amorphous and quenched PEN/PET blend samples at 10°C/min heating rate including glass transition temperatures, crystallization peak temperatures (T_c), and heats of melting (endo ΔH) and crystallization (exo ΔH). All temperatures in °C, ΔH in J g^{-1}, and ΔC_p in J g^{-1} K^{-1}

Blending temperature (°C)	285	285	285	285	260	260
Blending time	10 s	100 s	5 min	25 min	5 min	25 min
T_g (PET)	79.4	80.6	95.6	95.9	80.9	94.1
ΔC_p	0.1959	0.1806	0.3468	0.3276	0.2049	0.3558
ΔT_g (°C)	12	13	33.5	17	14.4	31
T_g (PEN)	120	118			118.2	
ΔC_p	0.1026	0.147			0.1269	
ΔT_g (°C)	11.4	14.5			14.1	
Exo ΔH_1 (PET)	14.3	15.9	34.7		16.4	28.4
T_{c_1} (°C)	138.1	143.8	169.8		143.2	167
Exo ΔH_2 (PEN)	20.3	22.7			23	
T_{c_2} (°C)	182	180.85			179.9	
Endo ΔH_1 (PET)	25.3	24.1	19.4		23.1	23.7
T_{m_1} (°C)	256.7	255.9	252.1		255.4	243.5
Endo ΔH_2 (PEN)	13.4	14.1	13.7		14.85	3.5
T_{m_2} (°C)	265.1	265.3	261.5		265.65	268.6
Total (ΔH)	4.1	− 0.4	− 1.6		− 1.45	− 1.2

300 s at this temperature two separate glass transitions are seen and they are almost identical to those of the pure components (Table 2). The highest melting peak in the 1500 s (260°C) scan is likely due to annealing during blending at 260°C causing a high melting PEN morphology. After 1500 s of mixing at 285°C, the degree of randomization of the copolymer is so high that the system is unable to crystallize during DSC heating; while after 1500 s at 260°C, the single sharp T_g proves that the system is miscible and single phase, but both components are seen to readily crystallize upon heating with the PET blocks apparently crystallizing to a larger extent. This is estimated from the proportion of high and low melting species in the endotherm. The blend made at 285°C (300 s) shows a reasonably high level of compatibility with a single broad glass transition. Our experience shows that it is not completely miscible unless a single sharp glass transition is measured [24,31]. Its ability to crystallize to a high degree proves that even with a highly blocky structure the system becomes miscible or almost miscible, consistent with a large body of literature [32–37].

5. Discussion

5.1. TMDSC studies of amorphous PEN

Although the large extent of recrystallization at temperatures above 150°C in initially amorphous polymers like PEN is well recognized [6,25–27], examining the total DSC curves there is little direct indication of the large degree of recrystallization that causes the high melting points in the initially amorphous PEN (Fig. 1). This is because of compensating endothermic and exothermic contributions above the 'cold crystallization' peak and TMDSC adequately resolves these so there no longer is a need for indirect estimations. The nonreversing curve in Fig. 1 illustrates the level of exothermic recrystallization between 200 and 270°C which is well above the nominal cold crystallization peak at 177°C. In TMDSC of many polymers, a reversing endothermic contribution usually occurs over a similar temperature range as the NR exotherm (e.g. Figs. 1, 2, 5 and 7). This type of reversing endotherm corresponds to crystals undergoing rapid melting with the heat flow in phase with the period of the temperature modulation [11,12]. These crystals are unstable and melt well below the thermodynamic melting point. The reversing endothermic and NR exothermic responses can be related and it is likely that the unstable species are prone to recrystallization, melting, recrystallization and so on, and it is possible that the same morphological regions undergo such cycling between melting and crystallization several times over the broad temperature ranges where the NR exothermic processes are detected. Other contributions include a rapid recrystallization phenomena related to 'molecular nucleation' [9,10] which contribute to the reversing endothermic signal in the typical thermal scanning TMDSC experiment.

5.2. Isothermally annealed PEN

TMDSC data for PEN illustrate the three main endothermic processes that must be considered in interpretation of the DSC data, although only two distinct endotherms are usually detected. Melting of secondary crystals is followed by recrystallization that broadly overlaps with melting of primary crystals, with a highest temperature broad endothermic response which is attributed to melting of the

recrystallized (or perfected) species [4,6,14]. A few recent studies have detected triple melting in standard DSC scans at 10°C/min with various isothermal crystallized samples of PEN from both the glass and melt [1,3,4]. Our previous work also considered multiple melting endotherms in polymers and used TMDSC to study the three main melting processes along with the corresponding aspects of reorganization [6,12,15]. The work also showed how TMDSC and complementary techniques are able separate time dependent and heat capacity related contributions in the melting and recrystallization region. In these results, because of overlapping exothermic recrystallization, the broad primary crystal melting contributes to a small shoulder in the reversing curves occurring at ~250°C in Fig. 2, and these cannot be resolved completely from the melting of recrystallized species which dominates above this temperature. As was discussed recently [4,6,12], this is also verified by independently measured melting points of the initially present primary crystals by the rapid heating rate technique. For example, the rapid heating rate melting point [4,6] ($T_{m,rapid}$) of PEN annealed 80 min (170°C) in Fig. 2 is 245°C, but this is far below the end of melting because of the DSC scanned induced recrystallization. $T_{m,rapid}$ for 18 h and 5 day annealed PEN is also 245 ± 5°C. Similar comparisons were made for oriented films of PEN in relationship to the TMDSC characterization [6]. With high degrees of DSC scan-induced recrystallization masking contributions of primary crystal melting, the standard DSC data lose their effectiveness in characterizing some of the initially present morphologies which may be important in understanding the material properties. TMDSC is constrained to relatively low heating rates so even with the additional information on recrystallization, some contributions of primary crystal melting are difficult to resolve completely in PEN (Fig. 2).

By varying the annealing time from short times to very long times at 170°C, the melting of the primary crystals (seen as a shoulder at ~250°C in the reversing signal) is enhanced and the low endotherm due to melting of secondary crystals is resolvable in the NR signal. When the annealing temperature is increased to 210°C (Figs. 4 and 5) the melting of secondary crystals does appear as a shoulder in the higher heating rates in Fig. 4 (standard DSC), but at the lowest heating rate exothermic recrystallization just after the annealing temperature mostly cancels the low endotherm in the total signal. The largest endotherm at high temperatures is due to the melting of recrystallized species. The suppression of recrystallization during DSC heating at high rates broadens and shifts downward in temperature this peak (Figs. 4 and 6) as was discussed previously by Denchev et al. [5]. When the annealing time is increased to 17 h at 210°C, the low temperature endotherm (melting of secondary crystals) is not fully resolvable in the total heat flow signal (Fig. 7). The longer time allows the primary and secondary crystals to grow and perfect leading to higher crystallinity. The lower temperature endotherm in the dual endotherm data in Fig. 6 is the combination of melting of primary and secondary crystals while the higher temperature peak is the melting of the perfected species (which merge into a single peak at the highest heating rate). The TMDSC NR signal in Fig. 7 resolves the secondary crystal melting (at 254°C) from the strong reversible melting contribution from primary crystal melting. The superheatable nature of secondary crystal melting [28] is what allows TMDSC to separate it into the NR signal as was discussed previously [12]. These results highlight the ability of TMDSC to detect the three main endothermic processes occurring in the samples, and illustrate the advantage over standard DSC. With increasing time at these annealing temperatures, the primary and secondary crystals still undergo substantial reorganization during DSC heating. This was also observed by Denchev et al. [5] as they studied effects of annealing time at similar isothermal crystallization temperatures.

For the higher temperature annealed samples, the crystal morphology developed at low undercoolings leads to different TMDSC results [4]. At 240°C (Fig. 8) and 265°C (Fig. 9), these melt-crystallized samples display a single endotherm because the crystal perfection is high as a result of the elevated temperature annealing. A single endotherm is present in the samples with most of the endotherm detected in the NR signal. The percent of NR melting increases from 50% (240°C, 30 min) to 90% (265°C, 5 days) with annealing temperature and time. The secondary crystals that do form under these conditions are superheatable [12,28] and their melting is pushed into the main (primary) melting endotherm and is not fully resolvable even with TMDSC. Buchner et al. [2] also observed single melting endotherms in high temperature annealed samples and concluded reorganization did not take place, and Denchev et al. [5] characterized high temperature annealed PEN samples with DSC and SAXS and found that the results could best be described by a single lamellar population.

5.3. Blends

There are several interesting questions which can be addressed by our blending studies with very fast and efficient mechanical mixing. At both melt blending temperatures of 260 and 285°C, we can prove for the first time that melt mixed PET and PEN are essentially completely incompatible. The proof is the finding that at early times the glass transitions are almost identical to those of the pure components (Table 2) even though the blends are transparent and well 'mixed'. To our knowledge no melt mixing study has shown evidence of 'complete' incompatibility because mixing efficiencies were poor enough that some transesterification reaction always occurred by the time a uniform domain dispersion was attained [33]. Melt mixing to ~1 μm or smaller domain sizes is so fast that it is complete within about 5 s at 260 and 285°C. This was proved earlier in the study of many high temperature

miscible polymer pairs [24,31]. Thus, the reaction rate driving rate miscibility is found to be much slower than the establishment of a uniform dispersion of uniform domains because the DSC data show that it takes about 5–7 min and about 25 min at 285 and 260°C, respectively to attain miscibility (Fig. 11). In other literature melt blending studies [32] with mechanical mixing at 50/50 concentrations, 2.5 and 5 min were needed for miscibility at 285 and 275°C, respectively. This is relativity consistent with our results for 50/50 blends. For solvent cast and then melt annealed 50/50 blends, times of 20 min [37] and 40 min [34] were needed for miscibility. Andresen and Zachmann [33] found 2–10 min for miscibility of solvent cast 30/70 blends. One can conclude from this that the continual regeneration of interphase in a mechanical mixing situation substantially speeds up the effective rate of transesterification, as opposed to the static melt annealing of solvent cast blends. As more interfacial area becomes available during melt mixing, the number of reacting species naturally increases.

6. Conclusions

At low isothermal crystallization temperatures (170 and 210°C), double and sometimes triple melting endotherms are observed in standard DSC. TMDSC and the data from the rapid heating rate melting point method provide additional evidence as to the influence of crystallization time with the system becoming slightly less metastable with annealing time. However, substantial recrystallization in the NR signal is still present at the longest times (Figs. 2 and 6). At the higher annealing temperatures (240 and 260°C), the TMDSC scans only display single melting endotherms at these low heating rates consistent with other literature.

Time dependence of melt blending with a novel small-scale rapid blending method showed the progression from completely incompatible but well dispersed PET and PEN homopolymers, to miscible blocky (crystallizable) copolymers formed at different rates depending on temperature due to transesterification, to finally noncrystallizable more random copolymers. The DSC and TMDSC data also characterized the melting and recrystallization properties of the blends showing many similarities with the homopolymers.

References

[1] Cheng SD, Wunderlich B. Macromolecules 1988;21:789.
[2] Buchner S, Wiswe D, Zachmann HG. Polymer 1989;30:480.
[3] Medellin-Rodriguez FJ, Phillips PJ, Lin JS. Macromolecules 1996;29:7491.
[4] Sauer BB, Kampert WG, Blanchard EN, Threefoot SA, Hsiao BS. Polymer 2000;41:1099.
[5] Denchev Z, Nogales A, Ezquerra TA, Fernandes-Nascimento J, Baltà-Calleja FJ. J Polym Sci, Polym Phys 2000;38:1167.
[6] Sauer BB, Kampert WG, McLean RS, Carcia PF. J Therm Anal Cal 2000;59:227.
[7] Reading M. Trends Polym Sci 1993;8:248.
[8] Reading M, Elliot D, Hill VL. J Therm Anal 1993;40:949.
[9] Okazaki I, Wunderlich B. Macromol Rapid Commun 1997;18:313.
[10] Okazaki I, Wunderlich B. Macromolecules 1997;30:1758.
[11] Thomas LT. Personal communication.
[12] Kampert WG, Sauer BB. Polym Engng Sci, submitted for publication.
[13] Wunderlich B. Macromolecular physics, vol. 3. New York: Academic Press, 1980.
[14] Zhou C, Clough SB. Polym Engng Sci 1988;28:65.
[15] Hsiao BS, Gardner KH, Wu DQ, Chu B. Polymer 1993;34:3986.
[16] Fougnies C, Damman P, Villers D, Dosiere M, Koch MHJ. Macromolecules 1997;30:1385.
[17] Fougnies C, Dosiere M, Koch MHJ, Roovers J. Macromolecules 1999;32:8133.
[18] T.A. Instruments Inc., Literature, New Castle, DE.
[19] Toda A, Tomita C, Hikosaka M, Saruyama Y. Polymer 1998;39:5093.
[20] Chen W, Toda A, Moon I-K, Wunderlich B. J Polym Sci, Polym Phys 1999;37:1539.
[21] Toda A, Arita T, Tomita C, Hikosaka M. Polymer 2000;41:8941.
[22] Wunderlich B, Boller A, Ozazaki I, Kreitmeier S. Thermochim Acta 1996;282/283:143.
[23] Merzlyakov M, Schick C. Thermochim Acta 2000;330:55.
[24] Sauer BB, Hsiao BS. Polymer 1993;34:3315.
[25] Holdsworth PJ, Turner-Jones A. Polymer 1971;12:195.
[26] Blundell DJ, Osborn BN. Polymer 1983;24:953.
[27] Blundell SD. Polymer 1987;28:2248.
[28] Marand H, Alizadeh A, Farmer R, Desai R, Velikov V. Macromolecules 2000;33:3392.
[29] Lee Y, Porter RS, Lin JS. Macromolecules 1989;22:1756.
[30] Lee Y, Porter RS. Macromolecules 1987;20:1336.
[31] Sauer BB, Hsiao BS, Faron KL. Polymer 1996;37:445.
[32] Stewart ME, Cox AJ, Naylor DM. Polymer 1993;34:4060.
[33] Andresen E, Zachmann HG. Colloid Polym Sci 1994;272:1352.
[34] Ihm DW, Park SY, Chang CG, Kim YS, Lee HK. J Polym Sci, Polym Chem 1996;34:2841.
[35] Guo M, Brittain WJ. Macromolecules 1998;31:7166.
[36] Rwei S-P. Polym Engng Sci 1999;39:2475.
[37] Collins S, Kenwright AM, Pawson C, Peace SK, Richards RW, MacDonald WA, Mills P. Macromolecules 2000;33:2974.